Natural Resources Canada | Ressources naturelles Canada

GEOLOGICAL SURVEY OF CANADA
OPEN FILE 8801

Uranium, thorium, and potassium analyses using pXRF spectrometry

R.D. Knight, B.A. Kjarsgaard, E.G. Potter, and A. Plourde

2021

Canada

GEOLOGICAL SURVEY OF CANADA
OPEN FILE 8801

Uranium, thorium, and potassium analyses using pXRF spectrometry

R.D. Knight, B.A. Kjarsgaard, E.G. Potter, and A. Plourde

2021

Permanent link: https://doi.org/10.4095/328973

This publication is available for free download through GEOSCAN (https://geoscan.nrcan.gc.ca/).

Recommended citation
Knight, R.D., Kjarsgaard, B.A., Potter, E.G., and Plourde, A., 2021. Uranium, thorium, and potassium analyses using pXRF spectrometry; Geological Survey of Canada, Open File 8801, 1 .zip file. https://doi.org/10.4095/328973

Publications in this series have not been formally edited; they are released as submitted by the author.

Table of Contents

Abstract

The application of portable XRF spectrometry (pXRF) for determining concentrations of uranium (U), thorium (Th) and potassium (K) was evaluated using a combination of 12 Certified Reference Materials, 17 Standard Reference Materials, and 25 rock samples collected from areas of known U occurrences or mineralization. Samples were analysed by pXRF in Soil, Mining Cu/Zn and Mining Ta/Hf modes. Resulting pXRF data were compared to published recommended values, obtained by total or near total digestion methods with ICP-MS and ICP-OES analysis.

Results for pXRF show a linear relationship, for thorium, potassium, and uranium (<5000 ppm U) as compared to the recommended concentrations. However, above 5000 ppm U, pXRF results show an exponential relationship with under reporting of pXRF concentrations compared to recommended values. Accuracy of the data can be improved by post-analysis correction using linear regression equations for potassium and thorium, and samples with <5000 ppm uranium; an exponential correction curve is required at >5000 ppm U. In addition, pXRF analyses of samples with high concentrations of uranium (e.g. >1 wt.% U) significantly over-estimated potassium contents as compared to the published values, indicating interference between the two elements not calibrated by the manufacturer software.

1.0 Introduction

Prospective geological settings for uranium deposits in Canada are often targeted using airborne geophysical techniques, followed by ground geophysics, boulder tracing, geochemical surveys and targeted drilling programs (e.g. Cameron, 1983; Jefferson and Delaney 2007; Potter and Wright, 2015; and references therein). In conjunction with these surveys, modern geologists have a plethora of portable, hand-held digital tools at their disposal including pXRF and gamma-ray spectrometry. Natural gamma-ray spectroscopy that produces K, *e*U and *e*Th concentrations is routinely used in exploration to detect uranium enrichment. The prefix "*e*" denotes that uranium and thorium concentrations are determined indirectly from their daughter products and assumed to be in secular equilibrium with the parent isotopes (Adams and Fryer, 1964). For uranium, ^{214}Pb or ^{214}Bi are generally used as indicators of ^{238}U, whereas ^{228}Ac rather than ^{212}Pb, ^{212}Bi, and ^{208}Tl, which are located to the later part of thorium decay series, is usually selected for ^{232}Th because of the second progeny and several gamma-rays with sufficient intensities (Ji et al., 2017). However, disequilibrium can occur in uranium deposits (particularly in sandstone deposits) where contrasting element mobility between uranium and its daughter radioisotopes of thorium, radium, and radon disrupts secular equilibrium (Marchais et al., 2020). Furthermore, a density correction for self-attenuation of low energy gamma-rays should be applied (Ji et al., 2017) which is a challenge when analyzing samples in a borehole or using a handheld gamma spectrometer where the effective sampling volume is approximately 25 cm depth and 1 m radius (IAEA, 2003). Gamma-ray self-absorption in uranium ores can also lead to non-linear relationships between gamma-ray counts and uranium concentrations greater than 1 wt.% U, with uranium contents underestimated by up to a factor 2.5 for a 50 wt. % uranium fraction (Carasco et al., 2018).

Portable X-ray fluorescence spectrometry (pXRF) is a cost effective real-time analytical tool capable of directly detecting and screening a suite of elements ranging from magnesium to uranium without relying on daughter products. Preliminary pXRF results reported by Tuovinen et al., (2015) using raw, unprepared rock samples indicate comparable results for uranium and thorium concentrations to data generated by gamma-ray spectrometry, alpha spectrometry and ICP-MS analysis. Furthermore, Proctor et al. (2020) report "good" correlations between pXRF and aqua regia ICP-MS data for soil samples.

The development of pXRF as a mainstream geochemical analytical method is summarized in Glanzman and Closs (2007), updated by Lemiere (2018), and compared with excellent results to traditional laboratory methods by Rouillon and Taylor (2016) and Knight et al. (2021). Ongoing advances in pXRF technology have resulted in the ability to collect geochemical data that would otherwise be beyond the financial scope of many projects where traditional laboratory geochemical analysis (i.e., comprehensive aqua regia, plus multi acid, plus fusion digestions followed by inductively-coupled plasma-mass spectrometry (ICP-MS/OES), can cost >$100/sample.

The objective of this open file is to report on the precision and accuracy of pXRF spectrometry for the analysis of uranium, thorium, and potassium. Uranium is the heaviest element in the periodic table capable of being quantified by pXRF spectrometry. We have examined a suite of Certified Reference Materials (CRM's), Standard Reference Materials (SRM's), and rock samples analyzed from areas of known uranium occurrences/mineralization to test the applicability of pXRF for U, Th, K analysis.

2.0 Background on pXRF spectrometry

Portable XRF spectrometry is a non-destructive surface to near-surface analytical technique that comprises an X-ray beam (emitted by interaction of an electron beam with an anode), a silicon-drifted detector (SDD), and an amplifier combined with a multi-beam analyzer to provide elemental abundances of the material being analyzed. The X-ray beam uses an energy source higher than the binding energy of electrons from the inner shells of atoms causing electrons to be displaced from the shell with the vacancy filled by an electron from an outer shell resulting in a loss of energy. This lost energy "fluorescence" is characteristic to each element (Potts and Webb, 1992). Resolution of the fluorescence process is dependent on pXRF manufacturer's propitiatory software to separate different energy levels and to minimize spectral interferences.

The pXRF spectrometer uses filter settings to differentiate elements by reducing energy interferences and minimizing the effects of energy peak overlaps. These filters utilize a combination of voltage, current, and a series of stacked metal foil plates placed between the X-ray tube and the sample to isolate specific regions of the energy spectrum. Each filter eliminates X-rays outside of a specific region of the energy spectrum that would otherwise contribute to background noise at the detector. A combination of filters and data processing algorithms (modes) are factory-calibrated for specific materials and expected concentrations being analyzed. For geological materials, common modes are 'Soil' and 'Mining'. Soil mode utilizes Compton normalization signal processing algorithm based on measured results of a certified standard versus the Compton peak produced from incoherent backscatter radiation. Soil mode is suited for element concentrations expected to occur with <1 wt.%, and includes elements that are often defined as trace elements.

Mining modes are used to detect elements expected to exceed 1 wt.% concentration (major elements) and utilizes 'Fundamental Parameters', an algorithm that applies X-ray physics to correct for overlapping peaks and matrix differences (Figura 1987; van Sprang 2000; Murphy et al., 2010). Mining mode can be custom configured by the manufacturer to target specific elements, such as Mining Cu/Zn or Mining Ta/Hf.

3.0 Background information for analyzed materials

The following samples were selected to evaluate the response of a pXRF spectrometer for analyses of potassium, uranium and thorium. The samples range from Certified Reference Materials (CRM'S), Standard Reference Materials (SRM's) and geological rock pulps. These samples cover a range in uranium concentrations from ~5 ppm U to ~25 wt. % U (Table 1).

3.1 Certified reference materials

BL-2a, BL-2b, BL-3 and BL-5: These certified reference materials were prepared by the Canada Center for Mineral and Energy Technology (CANMET) and represent ore mainly from the Fay mine with minor amounts from the Verna mine of Eldorado Nuclear Limited in Beaverlodge, Saskatchewan. The samples were dried at 100°C and ground to <74 µm. The samples consist of pitchblende in a mylonitized oligoclase-rich rock with hematite (BL-2a-CANMET Report 82-6E; BL-5-CANMET Report 79-4).

Table 1: List of recommended values for uranium.

Sample Number	Recommended Value (ppm U)	Recommended Value (ppm Th)	Recommended Value (ppm K)	Sample Number	Recommended Value (ppm U)	Recommended Value (ppm Th)	Recommended Value (ppm K)
14-PUA-25	250113	na	na	**UTS-3**	513	10	2600
PUA-19	245000	4.3	9000	**NIST 610**	462	457	461
60-16	137000	na	4100	**10-CQA-0566C2**	315	37	56800
PUA-37	129000	12.4	6000	**OKA-2**	219	28930	3400
PUA-70	103000	10.7	26000	**10-CQA-0553F5**	198	56.2	19800
PUA-71	103000	6.9	3000	**14-Till-1b**	95	5.6	17400
BL-5	70900	24.8	3800	**14-Till-4b**	92	14.6	24500
PUA-63	61700	3.4	3000	**DLH-7**	71	0.01	91
PUA-11	51700	10.5	21000	**10-CQA-0545B2**	62	411	32000
PUA-18	50000	31.8	8000	**UTS-2**	56	174	na
PUA-65	21700	13.4	13000	**14-Till-1c**	48	5.2	17300
BL-3	10200	15	6600	**14-Till-4c**	44	14.9	24700
PUA-68	9400	12.9	36000	**14-Till-1d**	32	5.2	17000
BL-2a	4260	13.6	6600	**14-Till-4d**	30	15.4	25300
11-PUA-012E3	3170	369	3900	**14-Till-1e**	25	5.2	18200
11-PUA-011F2	3090	27.3	39400	**14-Till-4e**	20	15.3	25500
10-CQA-0579E2	3010	95.7	39200	**14-Till-1f**	15	na	na
DH-1A	2629	910	14300	**14-Till-4f**	15	na	na
60-10	2040	na	31600	**LKSD-1**	9.7	2.2	9100
11-PUA-012E4	1730	224	12100	**Till-2**	5.7	18.4	254866
11-PUA-1000H1	960	90.2	41200	**Till-4**	5	17.4	26980

DH-1a: This sample is a uranium-thorium ore concentrate from Denison Mines Corporation in Elliot Lake, Ontario. The material is a sericitic feldspathic quartzite containing pyrite (10%), brannerite and uraninite. The sample was dried at 100°C and ground to <74 μm, (CANMET Report 81-11E).

LKSD-1: This sample represents sediment collected from the center of Joe Lake and Brady Lake, Ontario. The sample was blended and bottled at CANMET.

OKA-2: Britholite, a rare earth-, thorium-bearing silicate apatite, (CANMET Report 85-154) collected near Oka, Quebec by the radiation geophysics section of the GSC.

Till-1, Till-2, and Till-4: Sample Till-1 was collected 25 km northwest of Lanark, Ontario near Joe Lake. Till-2 was collected 5 km west of Sisson Brook, New Brunswick. Till-4 was principally collected in Sisson Brook, New Brunswick, however some molybdenite bearing soil from near Gatineau, Quebec was blended with the till prior to analyses in order to raise the molybdenum content (Lynch, 1996). Till-1 is silica matrix soil sample with a SiO_2 concentration of 60.9 wt.%, whereas Till-2 and Till-4 represents silica matrix glacial derived till with SiO_2 concentrations of 60.8 wt.% and 65.0 wt.%, respectively (Lynch, 1996).

UTS-2 and UTS-3: This tailings sample consists of a sericitic, feldspathic quartzite containing 10% pyrite. The sample was leached with sulphuric acid and treated with lime and limestone before disposal by Rio Algoma Ltd., in Elliot Lake, Ontario, (UTS-2 - CANMET Report NUTP-2E; UTS-3 - CANMET Report NUTP-2E).

CUP-2: CUP-2 is an ore concentrate from the Blind River refinery of Eldorado Resources Ltd., with reported values of 75.42 wt.% uranium (CANMET Report 81-11E). Other element concentrations reported for CUP-2 include (in wt.%): 0.80% S, 0.019% Ti, 0.62% Ca, 0.035% As, 0.311% Fe, 0.459% Na, 0.229% Mg and 0.11%K. CUP-2 was diluted with SiO_2 powder to create standard references materials with concentrations to occupy gaps in uranium data.

3.2 Standard reference materials

14-Till-1 and Till-4, b-e: These samples consist of CUP-2, an ore concentrate from the Blind River refinery of Eldorado Resources Ltd., diluted with Till-1 and Till-4 respectively to form predetermined concentrations of uranium as listed in Table 1.

14-PUA-10, -12.5, -15, -20A and -25A: This suit of samples consists of CUP-2 diluted with pure SiO_2 powder (>99.99 wt.% SiO_2) to form expected concentrations of 10, 12.5, 15, 20 and 25 wt.% uranium (Table 1).

DLH-7, DLH-10b: Silicate glass standard produced at the Pilkington Glass research laboratory in conjunction with the University of Manchester (England). DLH-7 elemental concentrations were determined by three independent laboratories using laser ablation ICP-MS (Hamilton and Hopkins, 1995). DLH-10b was powdered with an agate mortar and pestle for this study.

TCA-8010: A till sample from southern Manitoba, subsequently powdered. Data from aqua-regia and total fusion digestion analyses are reported in Girard et al. (2004).

NIST 610: Standard Reference Material glass produced by the National Institute for Standards and Technology (NIST) in the United States (Pearce et al., 1997; Jochum et al., 2011). It contains up to sixty-one trace elements at a nominal concentration level of 500 ppm.

3.3 Geological materials

60-10 and 60-16: These two samples consist of clay-altered sandstones from the Cigar Lake mine, Athabasca Basin, Saskatchewan.

09-PUA-11, -15, -18, -19, -22, -35, -37, -44, -63, -65, -68, -70, -71: This suit of samples consists of rock samples from Beaverlodge-Uranium City, Saskatchewan. The samples were prepared by lithium meta/tetraborate fusion followed by ICP-MS analysis at Act Labs in Ancaster (code 4 Litho). Samples with uranium contents exceeding the ICP-MS detection limits were followed up by X-ray fluorescence (XRF) assay. Analytical results are reported in Potter (in press).

09-PUA-11: high-grade uranium in amphibolite-facies metavolcanic rocks with hematite alteration and trace carbonate stringers from the Bolger open pit.

09-PUA-15: leucogranite with uranium-mineralized chlorite-quartz veinlets and vein breccias from the Eagle Claims U-Cu-Se showing.

09-PUA-18: uranium mineralized fine-grained leucogranite from the Eldorado Intermediate Zone.

09-PUA-19: uranium mineralized hematite-chlorite vein breccia with alkali feldspar clasts from the Gully Uranium Zone.
09-PUA-22: arkosic arenite from fault contact between leucogranite and the Martin Group at ABC mine site (U-mineralized & Chlorite veined).
09-PUA-35: amygdaloidal Martin Group basalt with <10cm wide calcite-pitchblende-chlorite-hematite veins from the Martin Lake Mine area.
09-PUA-37: hematite-altered, medium-grained basalt with trace carbonate-chlorite-pitchblende veinlets from the Martin Lake Mine area.
09-PUA-44: veinlets of chlorite-quartz-hematite+/-pitchblende in an altered quartzite contact between Murmac Bay group quartzite and Lodge Bay granite from the Kodiak Development showing.
09-PUA-63: carbonate-chlorite+/-pitchblende veinlets hosted in orthogneiss from the Don Lake Showings.
09-PUA-65: high-grade ore sample in highly altered Murmac Bay Group amphibolite from the Beta-Gamma Mine.
09-PUA-68: coarse-grained alkali feldspar granite with chlorite+/-pitchblende-lined fractures from the CC2 Concession showing.
09-PUA-70: high-grade uranium ore sample in Murmac Bay Group metasedimentary rock from the Cayzor Mine.
09-PUA-71: high-grade uranium ore in carbonate breccia with hematite altered, amphibolite clasts from the Cayzor Mine.

10-CQU-1665B2, 1665D3, -545B2, -553F5, -566C2, -579E2 and 11-PUA-1000H1, -11F2, -12E3, -12E4: These rocks are from iron oxide-copper-gold (IOCG) and affiliated prospects in the Great Bear magmatic zone, NWT. They were pulverized in an agate mill and analyzed using a near-total four acid digestion followed by ICP-MS (codes ME-MS61U & ME-MS-81U) at ALS laboratory Group in Vancouver, B.C. Full analytical results are reported in Corriveau et al. (2015).

10-CQA-1665B2: albite-altered metasiltstone crosscut by later K-feldspar-magnetite- hematite-uraninite veinlets and breccias from Lou Lake.
10-CQA-1665D3: albite-altered metasiltsone crosscut by later K-feldspar-magnetite-hematite-uraninte veinlets and breccias from Lou Lake.
10-CQA-545B2: coarse-grained alkali feldspar granite with fine-grained chlorite alteration and anomalous uranium and thorium from the Cole Lake complex.
10-CQA-553F5: amphibole-magnetite altered feldspar porphyry cross-cut by late, uranium-bearing, amphibole-rich shear zones at Fab Lake.
10-CQA-566C2: K-altered feldspar porphyry overprinted by amphibolite-magnetite veins, magnetite+pyrite alteration front and K-feldspar veinlets from Fab Lake.
10-CQA-579E2: feldspar porphyry with uraninite in intense magnetite-amphibole alteration from Fab Lake.
11-PUA-1000H1: altered amphibole-magnesium feldspar porphyry with crosscutting K-feldspar veinlets containing uraninite from Fab Lake.
11-PUA-11F2, -12E3, and -12E4: albite-altered metasiltsone crosscut by later K-feldspar-magnetite-hematite +/- uraninite veinlets and breccias from Lou Lake.

3.4 Blank samples

Teflon Blank is a solid ~8 mm thick disk of Teflon and does not contain any elements detectable by the pXRF.

SiO_2 DP6000 blank provided by Bruker Scientific and supplied as a blank sample with a Bruker SI Tracer IV GEO pXRF.

SiO_2-1 consists of a silicon dioxide powder provided by the sedimentology laboratory at the Geological Survey of Canada.

SiO_2-2 represents the silicon dioxide powder used to dilute uranium concentrations for samples 14-PUA-10, -12.5, -15, -20A and -25A.

4.0 Methods

Analyses were acquired using a handheld Thermo Scientific Niton XL3t GOLDD XRF spectrometer (Table 2) hard wired to a power source and mounted in a test stand (Fig. 1). The test stand provides optimum beam-sample-detector geometry and a relatively clean test environment as opposed to a hand-held, open environment analysis. The spectrometer is equipped with four filters: High and Main (50kv/40µA max), differentiated by filter material composition and thickness; Low (20kv/100µA max); and Light (8kv/200µA max). At the start and finish of each analytical session and after every ~25 samples the cleanliness of the test stand window and pXRF interface was ascertained through the analyses of a Teflon disk and up to three different sourced silica (SiO_2) powder blank samples. The Teflon disk does not require any film interface between the sample and the instrument, however the SiO_2 samples in plastic cups are covered 4 µm thick Chemplex® Prolene®film to separate the sample from the analytical window. When data for the SiO_2 or Teflon blank returned values for elements that should not be detected in greater than trace amounts, the operating environment (test stand) was purged with compressed air and wiped clean with methanol until analyses confirmed the operating environment was not contaminated (Knight et al., 2021).

Data were collected via two distinct research activities using a combination of Soil, Mining Cu/Zn, and Mining Ta/Hf analysis modes. Data collected from research activity 1 was part of a larger study (Knight et al., 2013) on precision, accuracy, instrument drift, dwell time optimization, and calibration of a pXRF spectrometer. Data for uranium, thorium, and potassium from that publication has been utilized here to augment data collected during research activity 2.

Table 2: Factory-set technical specifications of the NITON XL3t GOLDD pXRF spectrometer used in this study.

Manufacturer	Thermo Scientific
Model	NITON XL3t GOLDD
Design year	2008
Excitation source	Cygnet 2W Ag tube
Voltage and current	6-50kV 0-200 uA
Detector	XL3 25 mm^2 SDD
Throughput	180,000 cps
Spot size	8 mm^2 diameter (used in this study) can be culminated to 4 mm diameter

Figure 1. Bench mounted (closed system), pXRF operated via portable computer, with vials of samples in a box on the right hand side of the photo. Photograph by R.D. Knight. NRCan photo 2020-926.

4.1 Research activity 1 (Ra1) – pXRF: K, U, Th precision and accuracy

In order to examine precision and accuracy of pXRF results for uranium, thorium and potassium, and to ascertain potential spectrometer drift, CRM's/SRM's Till-2, NIST 610, DLH-7, and DLH-10b were repeatedly (continuously) analyzed in Soil mode for approximately 110 measurements each over a two day and a three day period. Analyses were carried out with a dwell time of 60 seconds for each of the Main, Low, and High filters. Powdered samples (Till-2, DLH-10b) were covered by a 6 μm thick SpectroCertified® Mylar® polyester sheet, whereas the glass standards (NIST 610, DHL-7) were placed directly on the test stand. Samples where not moved between analyses.

4.2 Research activity 2 (Ra2) – pXRF: K, U, Th concentration

This activity addresses a comparison of recommended values with pXRF data collected from our full set of 54 CRM's/SRM's and geological samples as listed in sections 3.1, 3.2 and 3.3 that comprise a broad range uranium, thorium, and potassium concentrations. Portable XRF data were acquired using three factory pre-set pXRF analytical modes: Soil mode, Mining mode Cu/Zn and Mining mode Ta/Hf, utilizing an un-collimated 8 mm window. Soil mode analyses were carried out with a dwell time of 60 seconds for each of the Main, Low, and High filters. For both Mining modes, analyses were carried out with a dwell time of 45 seconds for each of the Main, Low, High, and Light filters i.e. a total dwell time of 180 seconds. The silica blank, CRM's/SRMs', and geological powdered samples were placed in plastic vials prior to analyses and covered with 4 μm thick Chemplex® Prolene®film. For each mode, a single sample was analyzed twice in the test stand without moving the sample. After all of the 54 samples were analyzed, the process was repeated four times, resulting in eight analyses for each sample, for a total of 1549 analyses. In order to monitor potential daily drift, CRM's/ SRM's from the suite of 54 samples were further analysed at the start and end of each session and after every 25 analyses.

5.0 Results

Recommended values for uranium, thorium, and potassium for the 54 samples used in this study as well as sample material and sample type are shown in Table 1. Limits of detection for pXRF results with a matrix of SiO_2+Fe+Ca are shown in Excel Data tables as provided by Thermo Fisher Scientific (2010). It should be noted that the NITON pXRF on occasion reports a value lower than the limit of detection provided by Thermo Scientific. Results are organized in two folders: Research activity 1 and Research activity 2. Data acquired for Teflon and SiO_2 blanks are appended at the bottom of each CRM/SRM worksheet. The Teflon blank often returned low values for Mo, Ti, U, Zr in soil mode and Ag, Al, Ca, Cl, Mg, S, Si, and Th in Mining mode. The SiO_2 blanks often returned low values for Ag, Ba, Ca, Cd, Cs, Fe, K, Mn, Pd, Te, U, and V, many of which are listed as impurities in the Chemplex® Prolene®film.

Graphical illustrations and statistical analysis of the data including generation of regression lines where created using StatView 5® and imported to Adobe Illustrator® for publication purposes.

5.1 Research activity 1 – pXRF: K, U, Th precision and accuracy

Results are presented in two files: R1 data.xls and Ra1 graphs.pdf. Ra1 data.xls comprises an Excel® workbook with four worksheets, (one for each CRM/SRM) containing pXRF analytical data for uranium, thorium, and potassium that was used to create the graphs shown in file Ra1 graphs.pdf. At the base of each worksheet is a summary table listing the sample count, minimum value, maximum value, mean, standard deviation (Std dev), relative standard deviation (%RSD), limit of detection for pXRF data as provided by the manufacturer, and the recommended value for each sample as reported from published data of previous lab testing.

Ra1 graphs.pdf comprises an illustration of the Ra1 data.xls file with concentrations for uranium, thorium, and potassium on the y-axis and reading number for each analysis on the x-axis.

In general, pXRF results are precise, but can lack accuracy as shown in Figure 2 for thorium collected from NIST-610. For this sample, the mean concentration obtained from 125 analyses is 756 ppm Th as compared to the recommended value of 457 ppm Th. Data showing both precision and accuracy are shown for uranium, thorium, and potassium in Ra1 graphs.pdf.

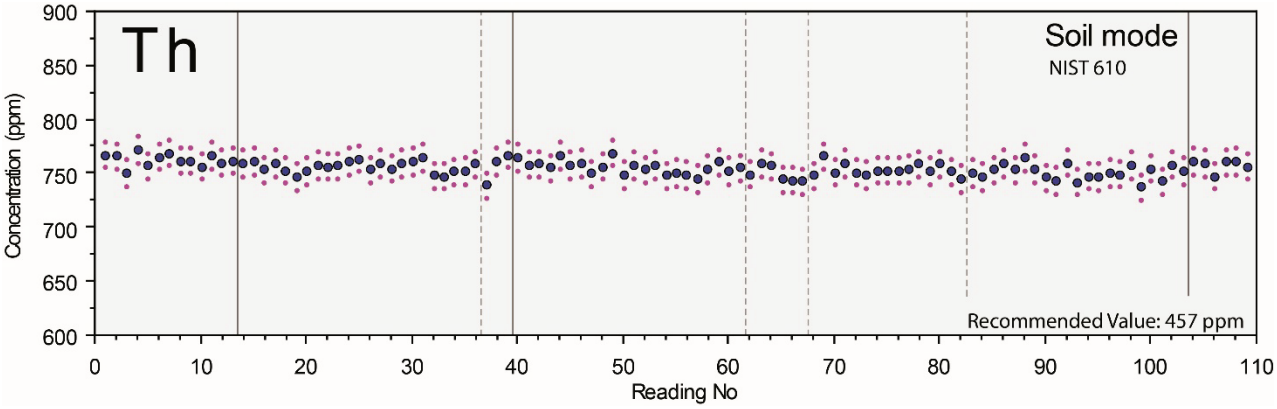

Figure 2. Thorium analyses for NIST-610 in Soil mode with a dwell time of 60 seconds per filter. Blue dots represent the analyses. Red dots represent an uncertainty of ±2σ. Solid vertical lines indicated when the spectrometer was turned off for a period of at least 12 hours. Dashed vertical lines indicated that the spectrometer was turned off for more than 20 minutes.

Results for uranium are less accurate. Precision for all CRM's/SRM' where time gaps between analyses as short as 30 minutes can result in large changes in concentrations. For Till-2, 106 analyses of uranium were collected over a three-day period where night gaps in time on Figure 3 are represented by solid vertical lines. For Till-2, uranium ranges from 6–22 ppm U with RSD of 30%; the recommended value is 5.7 ppm U. A single analysis (Reading #1) was collected approximately one month prior to the other analyses and shows a considerably higher concentration than the rest of the data. The first vertical dashed line located at analysis #44 represents a 30-minute time gap before continuing with further data collection. Not shown by vertical lines on Figure 4 are time breaks of 10 and 16 minutes, respectively, at analyses #28 and #35. It should be noted that the measurements of uranium in Till-2 are mostly below 20 ppm U

and sometimes below 10 ppm U; a 4 ppm limit of detection for the pXRF spectrometer is reported by Niton for a SiO_2+Fe+Ca matrix sample.

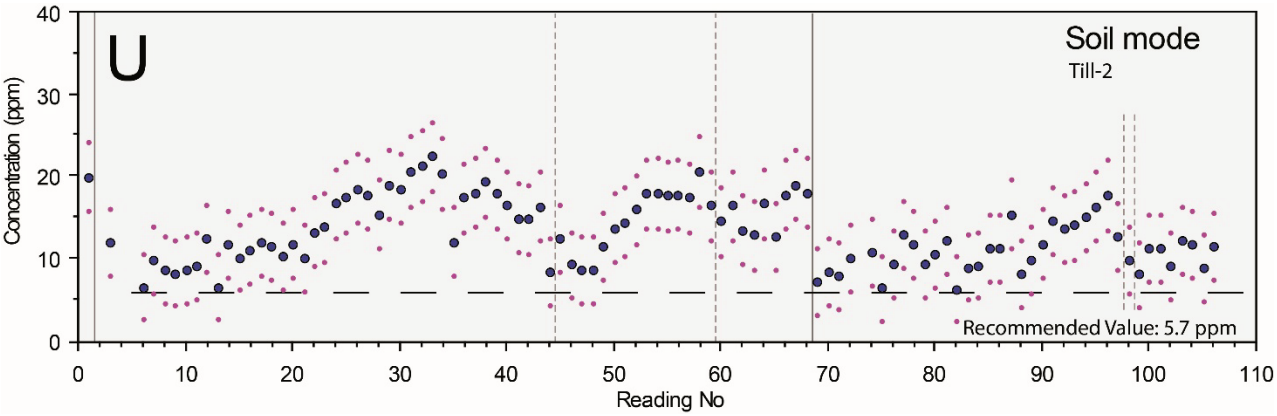

Figure 3. Uranium analyses for Till-2 in Soil mode with a dwell time of 60 seconds per filter. Blue dots represent the analyses. Red dots represent an uncertainty of ±2σ. Solid vertical lines indicated when the spectrometer was turned off for a period of at least 12 hours. Dashed vertical lines indicated that the spectrometer was turned off for more than 20 minutes.

For NIST 610, 111 analyses were acquired over a three-day period with a range in uranium values from 442–543 ppm U and a RSD of 2.8% (see Ra1 graphs.pdf); the recommended value is 462 ppm U (Table 1). For Till-2, NIST 610, BL-2, and DLH-10b, measured uranium contents increased with time until they were "reset" to lower values after a 30- to 90-minute time break between analyses. These results indicate that instrument drift for U occurred over the course of the analyses. These large shifts in concentration for uranium are also visible as coincident, but more subtle differences in measured concentrations of other elements. However, these are small fluctuations in terms of percent difference, and would likely be insignificant relative to inter-sample differences of a study. For example, the well-defined coincident U-K concentration drop measured in Till-2 between analyses #68 and #69 (see Ra1 graphs.pdf), for potassium represents only a ~2% decrease in concentration.

The behaviour of uranium may be influenced by heat build-up in the pXRF even with the instrument operating at a constant temperature controlled by a Peltier cooler. An examination of dates of analyses shows that no remarkable environmental conditions, such as temperature or humidity, can account for the abrupt changes in concentration that correspond to gaps in time between analyses. These data indicate that for uranium, data should be collected in as short a time frame as possible and that great control through multiple analyses of the same sample is crucial for a precise result. Using the pXRF to acquire a single analytical result for uranium could result in erroneous data for both precision and accuracy (see Ra1 graphs.pdf).

Table 3: Summary of research activity 2 data used to compare pXRF concentrations with recommended values (Recc). Data in red correspond to samples with anomalously high K concentrations determined by pXRF.

Sample I.D.	Material	Sample type	K Recc ppm	Th Recc ppm	U Recc ppm	K Soil ppm	Th Soil ppm	U Soil ppm	K CuZn ppm	Th CuZn ppm	U CuZn ppm	K TaHf ppm	Th TaHf ppm	U TaHf ppm
09-PUA-11	rock pulp	Beaverlodge - Uranuim City	21000	10.5	51700	37522	<LOD	16232	14338	<LOD	10699	14446	<LOD	10745
09-PUA-15	rock pulp	Beaverlodge - Uranuim City	16000	9.8	202000	62249	<LOD	26193	13394	<LOD	15261	13679	<LOD	15388
09-PUA-18	rock pulp	Beaverlodge - Uranuim City	8000	31.8	50000	23989	<LOD	15940	8071	<LOD	10529	8122	<LOD	10569
09-PUA-19	rock pulp	Beaverlodge - Uranuim City	9000	4.3	245000	63707	<LOD	27234	12575	<LOD	15632	13084	<LOD	15786
09-PUA-22	rock pulp	Beaverlodge - Uranuim City	3000	24.1	35500	18510	<LOD	13789	6263	<LOD	9335	6264	<LOD	9355
09-PUA-35	rock pulp	Beaverlodge - Uranuim City	na	0.3	21700	9144	<LOD	9589	2642	<LOD	6895	2560	<LOD	6859
09-PUA-37	rock pulp	Beaverlodge - Uranuim City	6000	12.4	129000	39286	<LOD	21459	9035	<LOD	13351	9230	<LOD	13362
09-PUA-44	rock pulp	Beaverlodge - Uranuim City	24000	2.4	19800	32650	75.86	11063	18694	<LOD	7783	18283	<LOD	7743
09-PUA-63	rock pulp	Beaverlodge - Uranuim City	3000	3.4	61700	28027	<LOD	19309	6730	<LOD	12233	6972	<LOD	12246
09-PUA-65	rock pulp	Beaverlodge - Uranuim City	13000	13.4	21700	17561	<LOD	10290	9196	<LOD	7241	9220	<LOD	7386
09-PUA-68	rock pulp	Beaverlodge - Uranuim City	36000	12.9	9400	40541	8.77	7375	29899	<LOD	5377	30227	<LOD	5367
09-PUA-70	rock pulp	Beaverlodge - Uranuim City	26000	10.7	103000	53762	<LOD	21092	16511	<LOD	13131	16495	<LOD	13137
09-PUA-71	rock pulp	Beaverlodge - Uranuim City	3000	6.9	103000	29404	<LOD	19807	6806	<LOD	12584	6877	<LOD	12621
10-CQA-0545B2	rock pulp	Great Bear magmatic zone	32000	411	62	32753	375	82	37072	415	68	37192	414	66
10-CQA-0553F5	rock pulp	Great Bear magmatic zone	19800	56.2	198	18590	38.68	158	20416	35.66	129	19746	34.81	129
10-CQA-0566C2	rock pulp	Great Bear magmatic zone	56800	37	315	56986	26.15	333	63379	12.91	250	61814	13.15	250
10-CQA-0579E2	rock pulp	Great Bear magmatic zone	39200	95.7	3010	36895	60.34	2763	33823	<LOD	2027	34260	<LOD	2061
10-CQA-1665B2	rock pulp	Great Bear magmatic zone	2300	88.9	880	3075	59.22	648	3065	<LOD	519	2807	<LOD	523
10-CQA-1665D3	rock pulp	Great Bear magmatic zone	2600	71.4	860	3477	48.98	767	3386	<LOD	628	3396	<LOD	608
11-PUA-1000.H1	rock pulp	Great Bear magmatic zone	41200	90.2	960	39956	52.06	833	42439	<LOD	682	42393	<LOD	651
11-PUA-11F2	rock pulp	Great Bear magmatic zone	39400	27.3	3090	78461	16	3209	75699	<LOD	2440	75202	<LOD	2448
11-PUA-12E3	rock pulp	Great Bear magmatic zone	3900	369	3170	5106	177	1582	4760	21.80	1270	4855	25.98	1239
11-PUA-12E4	rock pulp	Great Bear magmatic zone	12100	224	1730	13865	129	1112	14246	19.33	881	14247	22.29	896
60-10	rock pulp	Cigar Lake, Saskatchewan	31600	na	2040	62131	144	2268	64348	<LOD	1728	65243	<LOD	1717
60-16	rock pulp	Cigar Lake, Saskatchewan	4100	na	137000	29836	245	22514	8563	<LOD	13874	8780	<LOD	13793
BL-2a	CRM	CANMET	6600	13.6	4260	7910	10.53	3904	6869	<LOD	2978	6757	<LOD	2957
BL-2b	CRM	CANMET	na	16	4530	7952	10.95	3964	6904	<LOD	2973	6776	<LOD	2970
BL-3	CRM	CANMET	6600	15	10200	9159	11.97	7024	6198	<LOD	5077	6172	<LOD	5088
BL-5	CRM	CANMET	3800	24.8	70900	21443	<LOD	19027	5859	<LOD	11979	6054	<LOD	12074
DH-1a	CRM	Elliot Lake - ore	14300	910	2629	18321	763	2264	21180	514	1842	20690	521	1846
LKSD-1	CRM	CANMET	9100	2.2	9.7	9913	3.50	19	9485	9.57	11	9463	<LOD	26
OKA-2	CRM	OKA	3400	28930	219	7960	30302	278	38567	320	38	<LOD	38534	271
TILL-1	CRM	CANMET	18429	5.6	2.2	15557	4.19	9	16823	15.22	5	16673	15.76	5
TILL-2	CRM	CANMET	25486	18.4	5.7	22507	17.04	14	24411	22.67	8	24169	22.89	8
TILL-4	CRM	CANMET	26980	17.4	5	23811	42.39	14	25873	22.23	7	25730	22.28	7
UTS-2	CRM	Elliot Lake - tailings	na	174	56	21282	160	64	25367	157	56	26409	160	52
UTS-3	CRM	Elliot Lake - tailings	2600	10	513	2791	7.51	545	2729	<LOD	436	2716	<LOD	425
14-PUA-10	SRM	1.002 g CUP-2 diluted with 6.542 g SiO_2	200	213	101000	38489	27.80	24266	7081	<LOD	14515	6833	<LOD	14371
14-PUA-12.5	SRM	1.002 g CUP-2 diluted with 5.0336 g SiO_2	200	255	129500	48889	24.88	26086	8163	<LOD	15373	8110	<LOD	15285
14-PUA-15	SRM	1.002 g CUP-2 diluted with 4.028 g SiO_2	na	na	155500	52200	21.09	27143	8677	<LOD	15866	8785	<LOD	15756
14-PUA-20A	SRM	2.002 g CUP-2 diluted with 2.771 g SiO_2	na	na	200195	70873	15.68	29275	10430	<LOD	16712	10895	<LOD	16598
14-PUA-25A	SRM	2.002 g CUP-2 diluted with 2.0168 g SiO_2	na	na	250113	79199	14.33	30509	11788	<LOD	17213	11938	<LOD	17122
14-TILL-1b*	SRM	1.0015 g Till-1a combined with 9.7705 g Till-1	17400	5.6	95	17339	3.62	114	18917	<LOD	87	18825	<LOD	92
14-TILL-1c*	SRM	1.0015 g Till-1a combined with 20.5427 g Till-1	17300	5.2	48	16941	3.78	56	18923	11.06	36	18620	13.41	41
14-TILL-1d*	SRM	1.001 g Till-1a combined with 40.081 g Till-1	17000	5.2	32	16758	4.20	31	18933	11.02	23	18466	13.71	24
14-TILL-1e	SRM	5.2477 g Till-1d combined with 1.4998 g Till-1	18200	5.2	25	17056	3.78	26	19156	14.05	20	18648	13.33	19
14-TILL-1f	SRM	2.003 g Till-1d combined with 1.5001 g Till-1	na	na	15	16837	3.41	20	19441	10.93	14	18872	15.11	18
14-TILL-4b**	SRM	1.0015 g Till-4a combined with 9.4820 g Till-4	24500	14.6	92	26070	43.99	115	28718	12.53	93	28404	13.79	93
14-TILL-4c**	SRM	1.002 g Till-4a combined with 19.9628 g Till-4	24700	14.9	44	25994	44.02	51	29092	18.11	42	28328	19.57	45
14-TILL-4d**	SRM	1.001 g Till-4a combined with 41.918 g Till-4	25300	15.4	30	25752	44.43	28	28956	18.35	29	27910	20.84	28
14-TILL-4e	SRM	4.889 g Till-4d combined with 1.2605 g Till-4	25500	15.3	20	25591	42.88	28	29025	17.85	22	28472	22.54	25
14-TILL-4f	SRM	2.000 g Till-4d combined with 1.2591 g Till-4	na	na	15	25503	43.31	21	29426	19.85	19	28210	23.67	19
DLH-7	SRM	doped silicate glass	91	0.01	71	311	29.20	95	<LOD	<LOD	74	<LOD	<LOD	75
TCA-8010	SRM	GSC	19094	5.1	1.1	15979	3.94	8	17399	11.69	5	17277	11.71	5

* For the Till-1x series 74.4254 g Till-1 combined with 0.1064 g CUP-2 to create Till-1a

** For the Till-4x series 74.4205 g Till-4 combined with 0.1036 g CUP-2 to create Till-4a

5.2 Research activity 2 – pXRF K, U, Th comparison with recommended values

Numerical results for all elements detected by pXRF spectrometry are presented in an Excel® workbook (Ra2 data.xlsx) with three worksheets, one for each Soil, Mining Cu/Zn, and Mining Ta/Hf mode. The column next to each set of analyses contains the uncertainty associated with the analysis and corresponds to two standard deviations of the individual measurements taken throughout the 180 second analysis. Summary statistics for multiple analyses of each sample listing the sample count, minimum value, maximum value, mean, standard deviation, and %RSD are presented in rows under the sample analytical data. Data for Teflon and SiO_2 blank samples are included at the bottom of the Excel® table. A summary of data used to compare pXRF concentrations with recommended values is presented in Table 3.

Graphical illustration of the numerical data in the form of bivariate scatterplots are presented in Ra2 graphs.pdf, for uranium, thorium and potassium with the recommended sample concentration on the y-axis and concentration determined by pXRF analyses on the x-axis. For uranium and thorium, full data sets are shown on the top row of graphs with the second and third row having a change in maximum x-axis concentration to enlarge the data plots at lower concentrations. Plots for potassium show the full data set in each of the three pXRF modes and adjacent plots with outlies removed.

Uranium

In contrast to other elements determined by pXRF spectrometry that typically conform to a linear $y=mx \pm b$ relationship (Knight et al., 2021), uranium displays an exponential under-estimation for pXRF data as compared to recommended values obtained from laboratory methods, as illustrated for Soil mode in Figure 4 and both Mining modes (see Ra2 graphs.pdf). For soil mode, a closer examination of the bivariate plots from both 0 to 5000 ppm U (Figure 5) and 0 to 100 ppm U (Figure 6) display a linear $y=mx \pm b$ relationship that is near the 1:1 line (recommended values: pXRF). For concentrations up to 100 ppm U, both mining modes produce almost linear 1:1 results with very little offset on the x-axis as shown in Ra2 graphs.pdf; concentrations slightly over-estimated by pXRF. In contrast, concentrations from ~200 to 5000 ppm U are scattered, but slightly under-estimated by pXRF as compared to recommended values (Fig. 5). These variations may in part be due to matrix effects of the CRM's, SRM's and samples from mineralized occurrences. Both mining modes show similar results for the complete dataset. Note that our dataset does not contain samples with recommended concentrations ranging between 100 and ~200 ppm.

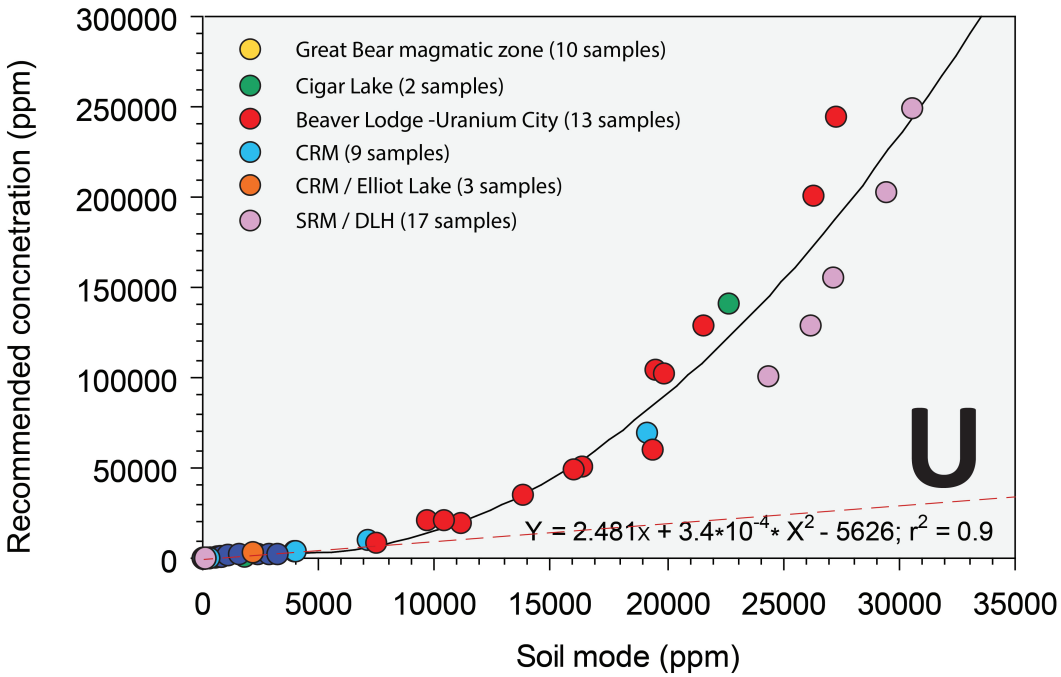

Figure 4. Uranium analyses by pXRF (x-axis) compared to recommended concentrations (y-axis). pXRF data display an exponential under-estimation compared to the recommended concentration. CRM= Certified Reference Materials; SRM = Standard Reference Materials. Note the difference in scale between x- and y-axis. Red dashed line equals a 1:1 relationship.

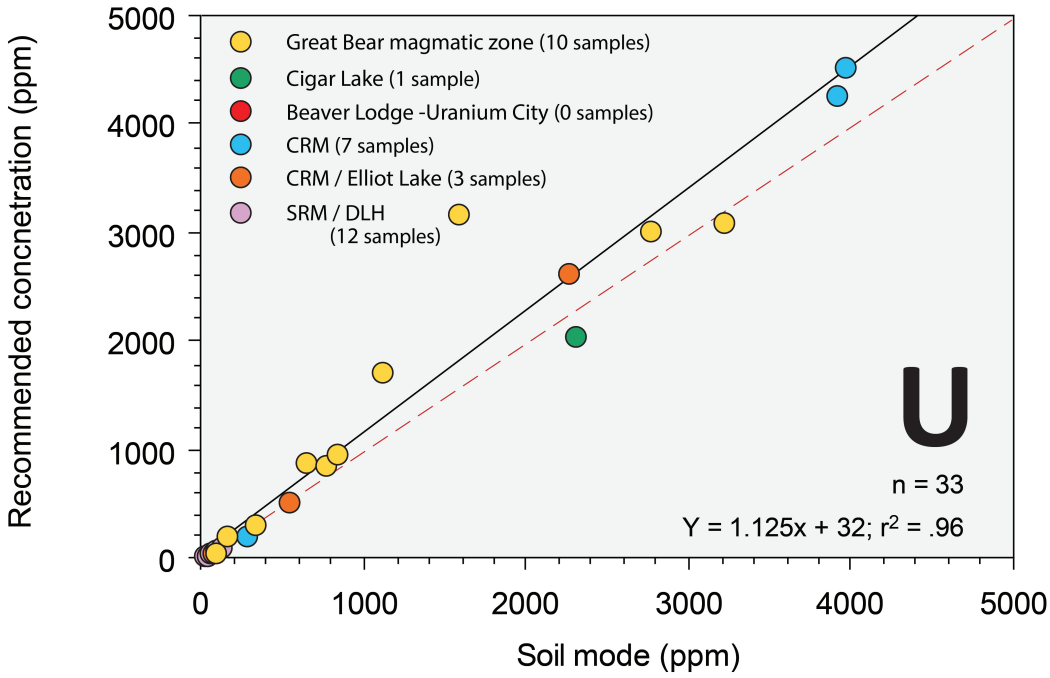

Figure 5. Enlargement of Fig. 4 from 0-5000 ppm. Data display a y=mx ± b relationship. Concentrations are slightly under-estimated by pXRF with greater under-estimation occurring as concentration increases. Red dashed line equals a 1:1 relationship.

Similar linear relationships are reported comparing an Olympus Vanta pXRF and ICP Assay methods for CRM's ranging up to 2000 ppm U (Olympus, 2021). Hass et al. (2017) report that uranium values obtained from a Cambrian-Ordovician sandstone aquifer in southern Wisconsin are accurate compared to ICP-MS for concentrations greater than 2 ppm U with their maximum reported concentration being 43 ppm U. Groover et al. (2017) compare pXRF uranium concentrations with traditional laboratory XRF methods for alluvium and rock samples from the western Mojave Desert. Their reported concentrations ranging from 2.8–180 ppm U also show a linear relationship. In an assessment of sedimentary phosphate deposits, Simandl et al. (2014) conclude that pXRF can identify RREs and zones enriched in uranium.

Collectively, these studies confirm that for uranium concentrations below ~200 ppm U, a linear relationship exists between pXRF data and with assay data. A comparison of uranium and thorium, from ore and mine tailings, using multiple methods are reported in Tuovinen et al. (2015). For values of uranium up to ~110 ppm U and thorium up to ~220 ppm Th, they conclude that pXRF data from unprepared samples show comparable results. For traditional laboratory-based X-ray fluorescence analyses, higher concentrations of uranium can result in a non-linear calibration curve that needs to be corrected by internal calibration (Suschny, 1992). In this study, we have calculated an exponential regression curve, for use with high U (> 5000 ppm) samples, that can be applied post-analysis.

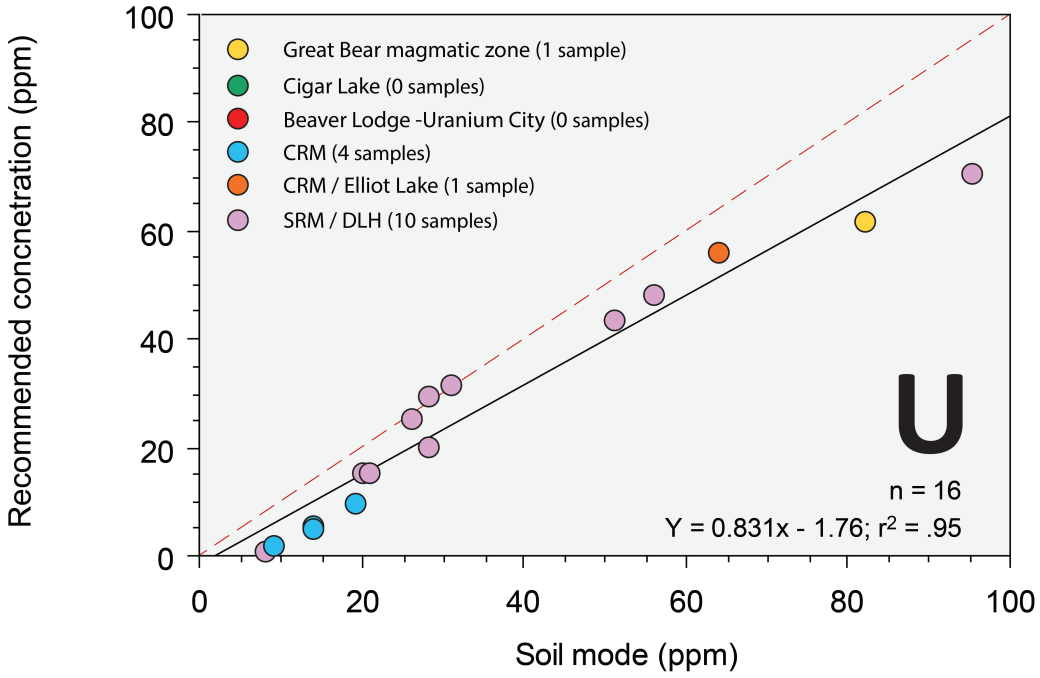

Figure 6. Enlargement of Figs 4 and 5 from 0-100 ppm. Data display a y=mx ± b relationship. pXRF concentrations are slightly over-estimated, with greater over-estimation occurring as concentration increases. Red dashed line equals a 1:1 relationship.

Thorium

The exponential relationship observed for uranium above ~5000 ppm U is not observed for thorium or potassium (Ra2 graphs.pdf). Note that the data set for thorium is small, as many of the samples concentration levels were below the limits of detection in Soil mode (4 ppm for a SiO2+Fe+Ca matrix), with no limits of detection listed for Mining modes. In all modes, analyses of three samples with reference values between 200 to 300 ppm Th show exceptionally poor relationships to pXRF data, with highly under estimated concentrations in Soil mode as shown in Figure 7. For the remaining data, there is a linear relationship, with pXRF slightly under-estimating the concentrations. pXRF also under-estimates concentrations for samples with under 30 ppm Th in Soil mode (Fig. 8), but over estimates concentrations in both Mining Cu-Zn and Mining Ta-Hf modes (see Ra2 graphs.pdf). Simandl et al. (2014) also report that thorium analyses by pXRF in Mining mode (35 ppm Th) over estimates concentrations compared to ICP-MS, although their data is exceptionally highly scattered resulting in $r^2 = 0.04$. Stanley et al. (2009) report a similar over-estimation of concentrations by pXRF compared to ICP-OES analyses from historic mine sites in Ireland and associated CRM's/SRM's. They suggest that a partial overlap of the thorium L_α line (12.97 keV) with the lead L_β line (12.61 keV) causes the over-estimation. In contrast, Hass et al. (2017) report that even with variable dwell times, thorium values of 1.24 - 11.15 ppm Th are near-equivalent to ICP-MS concentrations.

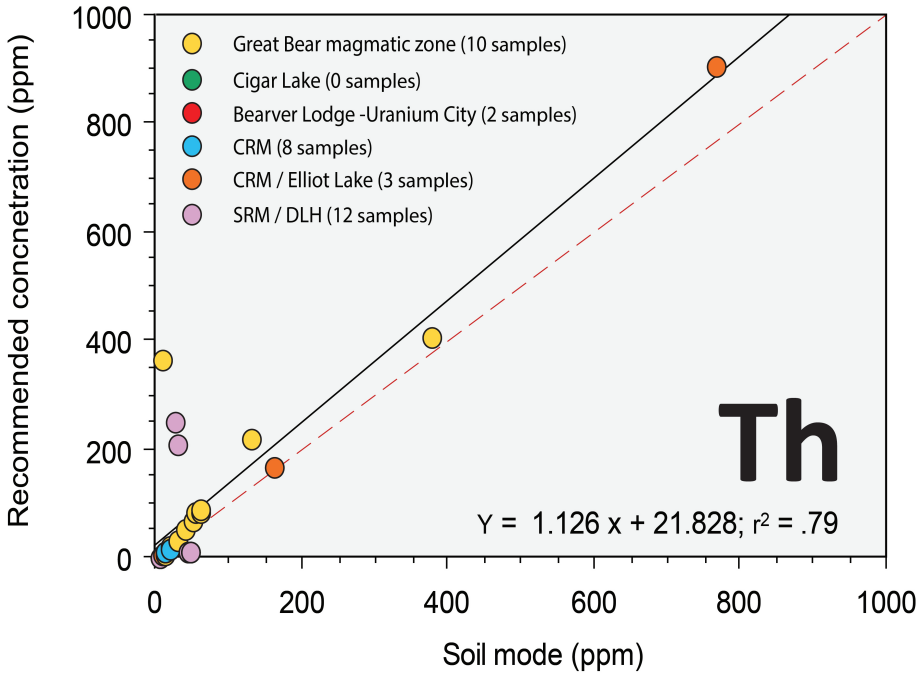

Figure 7. Thorium analyses by pXRF (x-axis) compared to recommended concentrations (y-axis). Three analyses between 200–300 ppm Th (recommended concentration) show a poor relationship with highly under-estimated concentrations by pXRF. Red dashed line equals a 1:1 relationship.

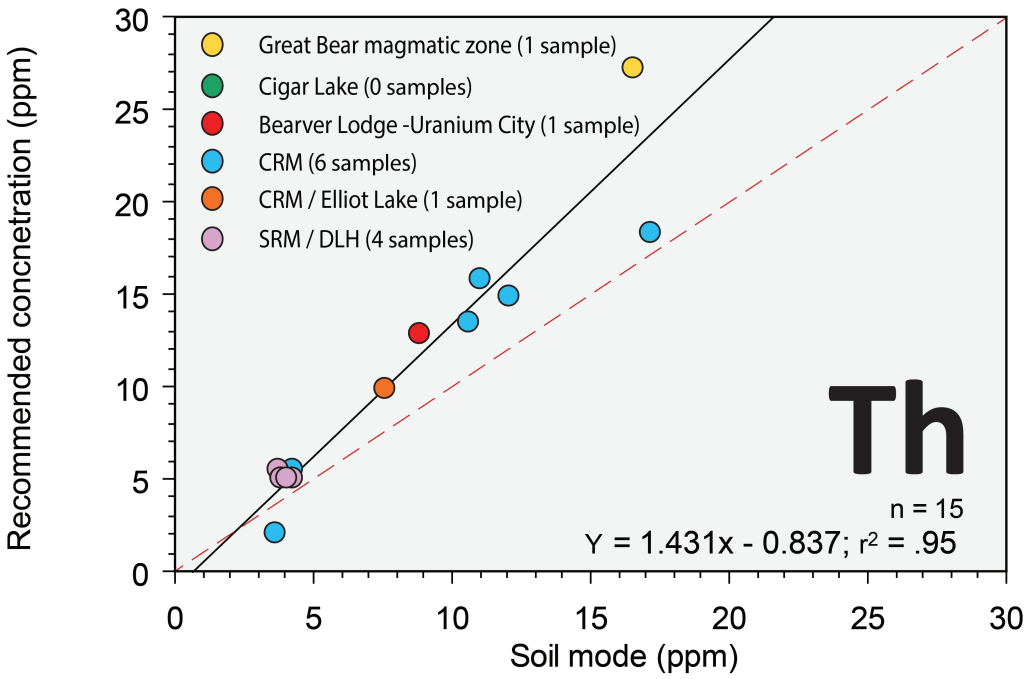

Figure 8. Enlargement of Fig. 8 from 0-30 ppm. For concentrations under 30 ppm Th, pXRF under-estimates concentrations. Red dashed line equals a 1:1 relationship.

Potassium

Bivariate scatterplots comparing recommended values for potassium with pXRF data are presented in Ra2 graphs.pdf as "a" and "b" plot sets. All data are represented in plot "a", with outliers removed in plot "b" (shown on the graph by grey circles), for determination of the revised r^2 regression line. Potassium determined in Soil mode shows a poor correlation with recommended values (Fig. 9, compare 1:1 line). Many of the data outliers are samples from Beaver Lodge-Uranium City and Cigar Lake mines, and one sample from the Great Bear Magmatic zone, but include 1 CRM and 2 SRM. These samples all returned significantly higher concentrations by pXRF, reducing the r^2 value to 0.23. The two SRM samples (14-PUA-10 and 14-PUA-12.5) returned values at the detection limits of 200 ppm K from commercial laboratories. Based on the amount of diluted CUP-2 added to each of these samples, the theoretical amounts of K in samples 14-PUA-10 and 14-PUA-12.5 should be 146 and 183 ppm K, respectively, as compared to measured pXRF values of 38489 and 48889 ppm in soil mode (Fig. 9, lavender circles on the x-axis). Furthermore, these two samples returned 7081 and 8163 ppm in Cu-Zn mode, and 6833 and 8110 ppm in Hf/Ta mode (Table 3). Eliminating two SRM's (14-PUA-10, 14-PUA-12.5), 1 CRM (BL-5), and 12 geological outliers from the dataset results in an excellent correlation between laboratory and pXRF data (Fig. 10, grey circles on the x-axis). Notably, these outliers (Table 3, highlighted in red) typically have high (> 35500 ppm) uranium contents, except for samples 11-PUA-11F2 and 60-10. The discrepancies between laboratory and pXRF results for these outlying samples brings into question a potential issues with the pXRF methodology, or interpretation of X-ray counts by the manufacturers proprietary software. Samples with high uranium concentrations and discrepancies with pXRF results may indicate a potential interference between potassium and uranium. Situm et al. (2020) discuss overlapping uranium Mα1 (3170.8 eV) and potassium Kα1 (3313.8 eV) XRF peaks that could lead to interference, as shown for sample 14-PUA-10 in Figure 11a. Neilson et al. (1977) also point out large potassium-uranium

(and possibly argon) interferences in ore samples using energy dispersive analyses in XRF that are illustrated in Figure 11b.

The scattering of samples with higher K concentrations in Soil mode (Fig. 9, right of the 1:1 line) is not reproduced in either Mining mode, as shown in Ra2 graphs.pdf. In Mining Cu/Zn mode sample 14-PUA-10 returned concentrations of 7081 and 6833 ppm K. In Mining Ta/Hf mode sample 14-PUA-12.5 returned concentrations of 8136 and 8100 ppm K. These values are considerably lower than concentrations reported for Soil mode, yet still almost two orders of magnitude greater than the commercial analyses and/or expected/calculated values. Sample 11-PUA-11F2 returned values from commercial laboratories that are almost half of the value returned by pXRF. These results are puzzling as potassium is an element that often falls into the excellent quantitative category for pXRF analyses (Knight et al., 2013). Results for both mining modes show fewer outliers with higher concentrations by pXRF than values returned in Soil mode (Ra2 graphs.pdf). Analyses of samples 14-PUA-10 and 14-PUA-12.5 using mining modes still returned values from pXRF analyses greater than the commercial laboratory concentrations, however concentrations determined by the mining modes are significantly lower than values determined by Soil mode (Ra2 graphs.pdf, pink circles on the x-axis).

For evaporitic rocks Eccles et al. (2009) show an over-estimation of potassium by pXRF compared to ICP-ES with r^2=0.8 and an x-axis offset. A similar over-estimation of potassium has been reported by Simandl et al. (2014). Furthermore, Hall et al. (2014) report that potassium concentrations, by pXRF analyses of CRMs, show a y=mx ± b relationship with an r^2= ~0.98 and an over-estimation of 3.5 times the recommended value. They suggest that their potassium results are over-estimated due to interference of the calcium Kα1 3.69 keV line on the potassium Kα1 3.31 keV line. Samples from their study contain up to 12% Ca. For sample 14-PUA-10 form our data (as shown in Figure 11) calcium contents (calculated and from commercial analyses) range from 0.08 to 0.16 wt.% Ca in samples 14PUA-10 and 14PUA-12.5, and we suggest at these concentration levels this Ca Kα1 peak overlap is unlikely to have any significant effects on the determination of potassium contents by pXRF.

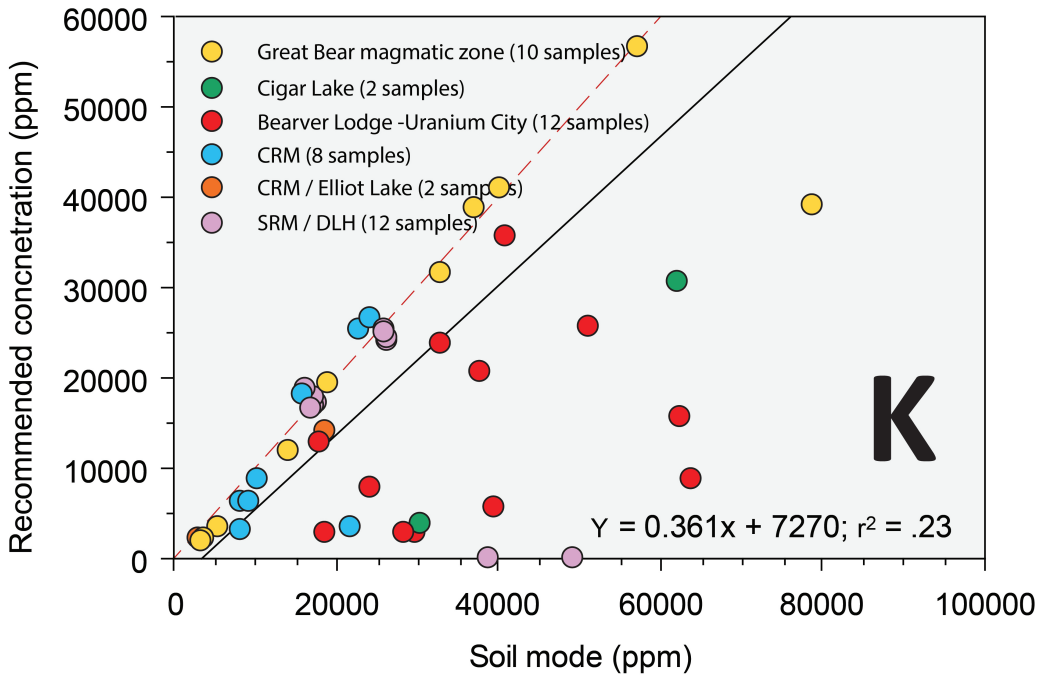

Figure 9. Potassium analyses by pXRF (x-axis) compared to recommended concentrations (y-axis). Numerous analyses by pXRF show poor correlation with recommended values. Data outliers associated with samples from Beaver Lodge-Uranium City, Cigar Lake, and one sample from the Great Bear Magmatic zone return significantly higher concentrations by pXRF reducing the r^2 value to 0.23. Red dashed line equals a 1:1 relationship.

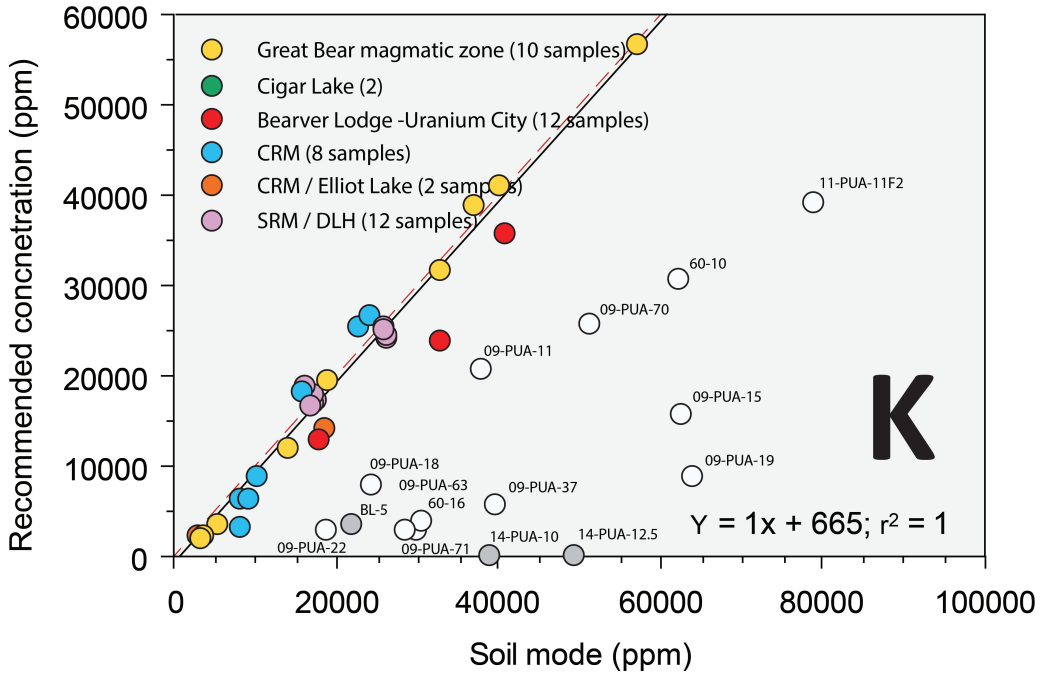

Figure 10. Geological samples with white circles and CRM/SRM samples with grey circles have been eliminated from the Fig. 9 dataset resulting in an excellent correlation with recommended values as shown by an r^2 value of 1. Red dashed line equals a 1:1 relationship.

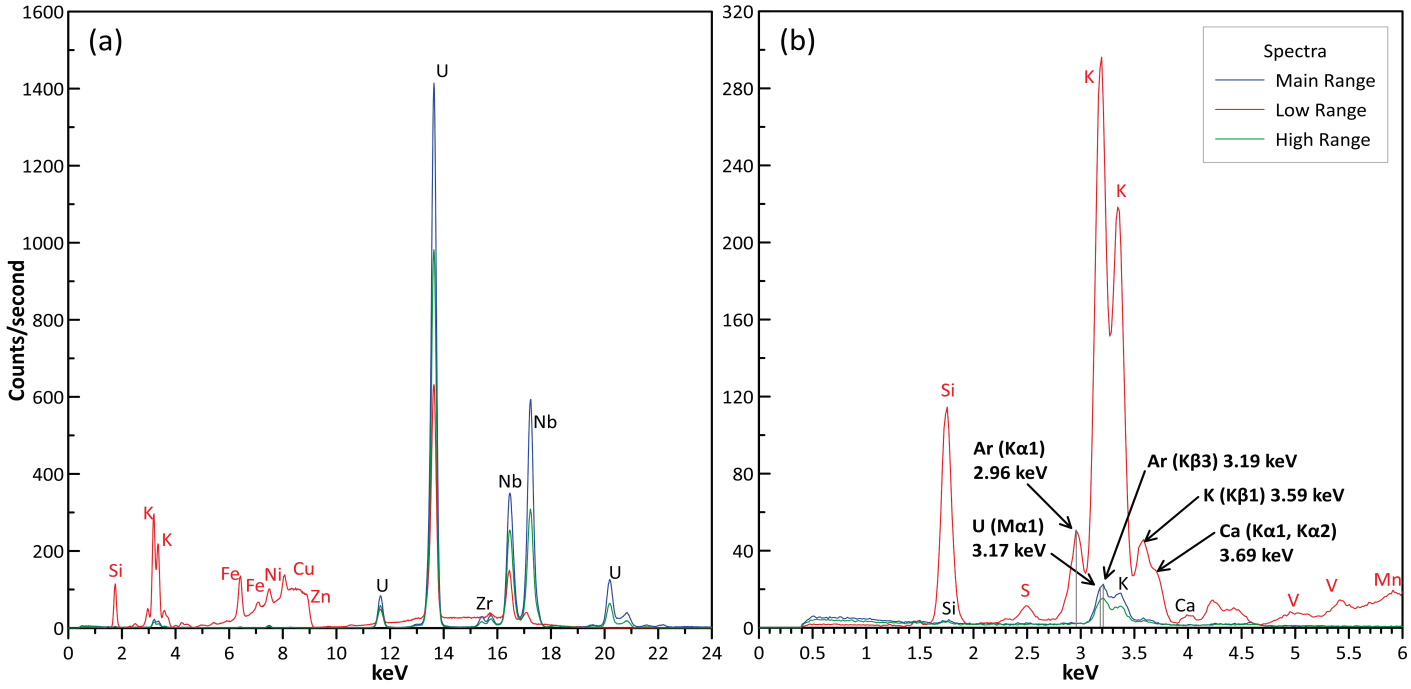

Figure 11. a) Energy peaks for sample 14-PUA-10. b) Low energy spectra of Figure 11a showing the potassium Kα1 3.31 keV peak overlapping with the uranium Mα1 3.17 keV and argon Kβ3 3.19 keV peaks, as well as overlapping potassium Kβ1, Kβ3 3.59 keV peaks with calcium Kβ1 3.59 keV and Kα1, Kα2 3.69 keV peaks.

6.0 Summary

A suite of Certified Reference Materials (CRM's), Standard Reference Materials (SRM's), and rocks collected from areas of known uranium enrichment were examined by pXRF spectrometry and compared with recommended values. For concentrations up to ~100 ppm U, pXRF consistently over-estimates uranium concentrations for sample materials analysed. The results also show that for concentrations from ~200 to ~5000 ppm U, pXRF slightly under estimates concentration, but a near linear 1:1 relationship with recommended values is maintained. An explanation for these discrepancies is yet to be determined. However, for traditional, lab-based XRF analyses, concentrations above 5000 ppm U analyses are exponentially under estimated, most likely due to due to self-absorption and must be corrected with a calibration curve. The under estimated concentrations can be adjusted for accuracy by calibration of the data using a regression equation.

Analysis of thorium contents by pXRF is variable. There is a linear relationship, with pXRF slightly under-estimating the concentrations, but that does not include 4 samples in which Th concentration by pXRF was highly underestimated, or over-estimated (1 sample). Potassium data showed significant discrepancies between laboratory results, theoretical values and pXRF data due to peak overlaps and interferences between uranium and potassium. Eliminating the outliers from the high-grade uranium deposits studied resulted in excellent correlation between laboratory and pXRF results.

Data collected in this study suggest that with careful analyses and understanding of the limitations in terms of site-specific mineral/element concentrations for both precision and accuracy, pXRF spectrometry is a valid method for sample screening to prioritize which samples to subject to additional laboratory analytical methods. As most exploration samples contain <5000 ppm U, pXRF spectrometry presents a cost effective method to rapidly asses and/or quantify (after calibration) uranium contents where secular disequilibrium, variable sample densities (e.g. intense hydrothermal alteration), or limited sampling volumes (i.e. drill core or hand samples) may impact quantification by portable gamma-ray spectrometry. However, in the hands of an inexperienced pXRF analyst and/or interpreter, the potential for collecting non-precise and inaccurate data is high, especially if "spot checks" are part of the data collection. For uranium analysis by pXRF spectrometry, it is vital that subsequent laboratory results verify the precision of the data and calibrate the pXRF data for accuracy. Furthermore, the development and application of a Mining mode specific calibration for uranium-rich samples to correct for overlapping peaks and matrix differences should increase the practicability of using this technique for exploration purposes.

7.0 Acknowledgements

Special thanks to Heather Crow for a technical review of the Open File. Data was collected as part of the Targeted Geoscience Initiative (TGI) Program, Geological Survey of Canada, Natural Resources Canada.

8.0 References

Adams, J.A.S. and Fryer, G.E., 1964. Portable Gamma-ray Spectrometer for Field Determination of Thorium Uranium and Potassium in The Natural Radiation Environment, University of Chicago Press, pp. 577-596.

Cameron, E.M. (ed) 1983. Uranium exploration in Athabasca Basin, Saskatchewan, Canada. Geological Survey of Canada, Paper 82-11, p. 71–110.

Carasco, C., Perot, B., Ma, J.-L., Toubon, H., Dubille-Auchere, A. 2018. Improving gross count gamma-ray logging in uranium mining with the NGRS probe. IEEE Transactions on Nuclear Science, v. 65, p. 919–923.

Corriveau, L., Lauzière, K., Montreuil, J.-F., Potter, E.G., Hanes, R., and Prémont, S., 2015. Dataset of geochemical data from iron oxide alkali-altered mineralising systems of the Great Bear magmatic zone, Northwest Territories. Geological Survey of Canada, Open File 7643, 1 .zip file. doi:10.4095/296301

Eccles, D.R., Al-Souqi, M., Gratten, K., and Dufresne, M.B., 2009. Preliminary investigation of Potash potential in Alberta. Energy Resource Conservation Board/Alberta Geological Survey, Open File Report 2009-20, p. 29.

Figura, P.M. 1987. Standardless quantitative X-ray fluorescence analysis using stored calibration constants. American Laboratory, v. 19, p. 156-164.

Girard, I., Klassen, R. A. and Laframboise, R. R. 2004. Sedimentology Laboratory Manual, Terrain Sciences Division. Geological Survey of Canada, Open File 4823; CD-ROM.

Glanzman, R.K. and Closs, L.G. 2007. Field portable x-ray fluorescence geochemical analysis – its contribution to onsite real-time project evaluation. in Proceedings of Exploration 07: Fifth Decennial International Conference on Mineral Exploration, 291–301.

Groover, K.D. and Izbicki, J.A., 2019. Selected trace-elements in alluvium and rocks, western Mojave Desert, southern California. Journal of Geochemical Exploration, v. 200, p. 234–248.

Hall, G.E.M., Bonham-Carter, G.F., and Buchar, A., 2014. Evaluation of portable X-ray fluorescence (pXRF) in exploration and mining: Phase 1, control reference materials. . Geochemistry: Exploration, Environment, Analysis, v.14, p. 99–123.

Hamilton, D.L. and Hopkins, T.C., 1995. Preparation of glasses for use as chemical standards involving the coprecipitated gel technique. Analyst, v. 120, p. 1373-1377.

Hass, L., Zambito, J., and Hart, D., 2017. Portable X-ray fluorescence (pXRF) measurements of Uranium and Thorium in Madison, Wisconsin, Water Utility Well 4 and 27. Wisconsin Geological and Natural History Survey, Open-File Report 2017-01, 21 p.

IAEA 2003. Guidelines for radioelement mapping using gamma ray spectrometry data. International Atomic Energy Agency, Vienna, TECDOC 1363, 179 p.

Jefferson, C.W. and Delaney, G. (eds) 2007. EXTECH IV: geology and uranium EXploration TECHnology of the Proterozoic Athabasca Basin, Saskatchewan and Alberta. Geological Survey of Canada Bulletin, 588, p. 489–506.

Ji, YY., Lim, JM., Kim, H. et al. 2017. Limitations of gamma-ray spectrometry in the quantification of 238U and 232Th in raw materials and by-products. Journal of Radioanalytical Nuclear Chemistry, v. 311, p. 1163–1168. https://doi.org/10.1007/s10967-016-4978-z

Jochum, K.P., Weis, U., Stoll, B., Kuzmin, D., Yang, Q., Raczek, I., Jacob, D.E., Stracke, A., Birbaum, K., Frick, D.A., Günther, D., and Enzweiler, J., 2011. Determination of Reference Values for NIST SRM 610-617 Glasses Following ISO Guidelines. Geostandards and Geoanalytical Research, v. 35, p. 397–429.

Knight, R.D., Kjarsgaard, B.A., Plourde, A.P., and Moroz, M. 2013. Portable XRF spectrometry of standard reference materials with respect to precision, accuracy, instrument drift, dwell time optimization, and calibration. Geological Survey of Canada, Open File 7358, 45 p. https://doi.org/10.4095/292677.

Knight, R.D., Kjarsgaard, B.A., and Russell, H.A.J., 2021. An analytical protocol for determining the elemental chemistry of Quaternary sediments using a portable X-ray fluorescence spectrometer. Applied Geochemistry, v. 131, p. 1–15.

Lemiere, B. 2018. A review of pXRF (field portable X-ray fluorescence) applications for applied geochemistry. Journal of Geochemical Exploration, 188: 350–360. https://doi.org/10.1016/j.gexplo.2018.02.006.

Marchais, T., Perot, B., Carasco, C., Ma, J-L., Allinei, P-G., Toubon, H., Goupillou, R., Collot, J. 2020. The use of self-induced X-ray fluorescence in gamma-ray spectroscopy of uranium ore samples. EPJ Web of Conferences 225, 05003. https://doi.org/10.1051/epjconf/202022505003.

Murphy, R.V., Maharaj, H., Lachapelle, J., and Yuen, P.K. 2010. Operator of portable X-ray fluorescence analysers, certification information and examination preparation booklet. Natural Resources Canada, Government of Canada.

Neilson, K.K., Wogman, N.A., Brodzinski, R.L. 1977. X-ray fluorescence capabilities for uranium ore analysis. U.S. Department of Energy, 17 p.

Olympus, 2021. Portable XRF for rare-earth element identification and exploration: application notes. p. 7. https://www.olympus-ims.com/en/applications/portable-xrf-for-rare-earth-element-identification-and-exploration/

Pearce, N.J.G., Perkins, W.T., Westgate, J.A., Gorton, M.P., Jackson, S.E., Neal, C.R., and Chenery, S.P. 1997. A compilation of new and published major and trace element data for NIST SRM 610 and NIST SRM 612 glass reference materials. Geostandards Newsletter, Journal of Geostandards and Geoanalysis, v. 21, p. 115–144.

Potts, P. J. and Webb, P. C. 1992. X-ray fluorescence spectrometry. Journal of Geochemical Exploration, v. 44, p. 251–296. https://doi.org/10.1016/0375-6742(92)90052-A.

Potter, E.G., in press. Geochemistry of uranium-bearing veins from the Uranium City-Beaverlodge district, northern Saskatchewan; Geological Survey of Canada, Open File 7873.

Potter, E.G., and Wright, D.M. (ed.), 2015. Targeted Geoscience Initiative 4: unconformity-related uranium systems. Geological Survey of Canada, Open File 7791, 126 p. doi:10.4095/295776

Proctor, G., Wang, H., Larson, S.L., Ballard, J.H., Knotek-Smith, H., Waggonor, C., Unz, R., Li, J., McComb, J., Jin, D., Arslan, Z., Han, F., 2020. Rapid Screening for Uranium in Soils Using Field-Portable X-ray Fluorescence Spectrometer: A Comparative Study. ACS Earth and Space Chemistry, v. 4, p. 211−217. https://dx.doi.org/10.1021/acsearthspacechem.9b00272

Rouillon, M. and Taylor, M. 2016. Can field portable X-ray fluorescence (pXRF) produce high quality data for application in environmental contamination research? Environmental Pollution, 214: 225-264. https://doi.org/10.1016/j.envpol.2016.03.055.

Simandl, G.J., Fajber, R., Paradis, S., 2014. Portable X-ray fluorescence in the assessment of rare earth enriched sedimentary phosphate deposits. Geochemistry: Exploration, Environment, Analysis, v. 14, p. 161-169. http://dx.doi.org/10.1144/geochem2012-180.

Situm, A., Beam, J.C., Hughes, K.A., Rowson, J., Crawford, A., Grosvenor, A.P. 2020. Analysis of low concentration U species within U mill tailings using X-ray microprobe. Journal of Electron Spectroscopy and Related Phenomena 244, 146992. https://doi.org/10.1016/j.elspec.2020.146992

Stanley, G., Gallagher, V., Ní Mhairtín F., Brogan, J., Lally, P., Doyle, E., and Farrell, L. 2009. Historic mines site - inventory and risk classification. Geochemical characterization and environmental matters - Appendix 4-XRF analyser, Assessment of analytical performance of NITON XLt 792Y field-portable analyser. Geological Survey of Ireland, 1: 40 p.

Suschny, O. 1992. Analytical chemistry of uranium. Analytical Techniques in Uranium Exploration and Ore Processing, IAEA Technical Report Series No. 341, p. 19–26.

Thermo Fisher Scientific, 2010. Thermo Fisher Scientific: Niton Analyzers, XL3t Analyzer, Version 7.0.1, User Guide, Revision C, elemental limits of detection in SiO_2 and SRM matrices using soil and mining analysis.

Tuovinen, H., Vesterbacka, D., Pohjolainen, E., Read, D., Solatie, D., Lehto, J. 2015. A comparison of analytical methods for determining uranium and thorium in ores and mill tailings. Journal of Geochemical Exploration, v. 148, p. 174–180. http://dx.doi.org/10.1016/j.gexplo.2014.09.004.

van Sprang, H.A., 2000. Fundamental parameter methods in XRF spectroscopy. 2000. Advances in X-ray Analysis, v. 42, p. 1-10.